A Brief Introduction to Noise Spectroscopy via Filter Functions*

David Rower†
Physics Department, Massachusetts Institute of Technology
(Dated: September 22, 2020)

The coupling of quantum systems to external degrees of freedom is a double-edged sword. On one hand, the coupling can lead to uncontrolled dissipative evolution of the system and the uninvited loss of phase information, in other words, decoherence. On the other hand, quantum systems can be utilized as sensitive probes to gain insights about the external degrees of freedom. In this term paper, we introduce one of the workhorse tools used to explore these ideas - noise spectroscopy with filter functions. This technique involves measuring the coherence of a qubit under the influence of different pulse sequences, effectively adjusting the sensitivity of the qubit to noise at different frequencies. We present a formalism of these ideas and highlight some recent results enabled by this technique in exploring the noise seen by nitrogen-vacancy (NV) centers and superconducting qubits. We conclude with an outlook on the field of noise spectroscopy.

I. INTRODUCTION

As the quantum revolution blossoms, the search for a platform to realize pristine, tunable, coupled two-level systems has become a race. This race has motivated rapid progress in the field of quantum control for a number of different physical systems ranging from the photonic to the solid-state. Each platform comes with benefits and disadvantages, many of which derive from how the physical qubits couple to their environment. In the case of building a long-lived quantum memory or information processor, this coupling is unwelcome. However, in the case of building a quantum sensor, this coupling is embraced. In all scenarios, it is clear that understanding environmental noise will pave the way to engineering more robust and useful quantum systems.

But how does one explore environmental noise in quantum systems? The field of noise spectroscopy, where qubits are used to measure the spectra of stochastic signals [1], has provided an answer to this question. The techniques of noise spectroscopy have enabled breakthroughs in the microscopic understanding of noise seen in many kinds of quantum systems, some recent examples being charge, flux, and frequency noise in superconducting qubits [2–4], and noise in NV center qubits [5, 6].

We introduce the reader to noise spectroscopy via filter functions. In Section II, we present the formalism of coherence and filter functions, and feature some canonical pulse sequences and noise spectra. In Section III, we present some applications of the discussed ideas to extracting and understanding the nature of noise seen by NV center and superconducting qubits. In Section IV, we give an outlook on the field of noise spectroscopy. We hope the reader will take away a first-principles understanding of the presented methodology of noise spectroscopy via filter functions, an appreciation for the results it has enabled, and an excitement for the future of quantum science and technology.

II. FORMALISM OF QUBIT COHERENCE

A. System Hamiltonian

In order for us to explore an environment via a qubit with ground and excited states $|g\rangle$ and $|e\rangle$, we must develop a model of the qubit-environment coupling. For completeness, we begin with a total Hamiltonian composed of the internal qubit Hamiltonian H_{qb}, the qubit-environment interaction Hamiltonian H_{I}, and the internal environment Hamiltonian H_{env},

$$H = H_{\mathrm{qb}} + H_{\mathrm{I}} + H_{\mathrm{env}}. \tag{1}$$

The effect of H_{env} can be explicitly considered with a master equation approach [7] by performing a partial trace over the environment states, or implicitly with a semi-classical approach by introducing an effective interaction Hamiltonian which lives in the qubit Hilbert space and contains stochastic coupling strengths: H_{I}' [8]. We present the latter formulation, which provides us with a Hamiltonian

$$H = H_{\mathrm{qb}} + H_{\mathrm{I}}'. \tag{2}$$

We now consider the problem of pure-dephasing, where the interaction H_{I}' only contains a longitudinal coupling term: $H_{\mathrm{I}}' \propto \sigma_z$. This is realized when the energy relaxation time of the qubit (T_1) is much longer than the dephasing time of the qubit (T_2), as is the case in many experimental systems. Explicitly, we consider the system

$$H = \frac{\hbar}{2}\left(\omega_0 + \eta(t)\right)\sigma_z, \tag{3}$$

where $\eta(t)$ is a stationary process describing the stochastic energy shift of the qubit induced by the environment. This process is characterized by an autocorrelation function $G(\tau)$ and power spectral density (PSD) $S(\omega)$:

$$G(\tau) = \langle\, \eta(t+\tau)\, \eta(t)\, \rangle, \tag{4}$$

$$S(\omega) = \int_{-\infty}^{\infty} e^{i\omega t}\, G(t)\, dt. \tag{5}$$

---

* An 8.421 Term Paper
† rower@mit.edu

It is important to recognize the distinction between the noise amplitude $\eta(t)$ and dynamics $G(\tau)$. This distinction can be subtle, so we present an intuitive example in the context of surface spins providing magnetic field noise to an NV qubit. If we suppose the number of electron spins on the surface changes from experiment to experiment, the amplitude of $\eta(t)$ will vary. However, during any particular experiment (*e.g.* measuring the excited state population at a specific time), the dynamics of the noise $G(\tau)$ will only depend on the relevant physics of dipolar interactions. From this argument, we see that the distribution of amplitudes of $\eta(t)$ can be distinct from the autocorrelation function $G(\tau)$.

B. Derivation of the Coherence Function

The region of the spectrum $S(\omega)$ that the qubit is sensitive to can be tuned by modulating the phase of the qubit at specific times with a pulse sequence, in turn changing the phase accumulated by the qubit as it evolves under $\eta(t)$. The power of noise spectroscopy via filter functions comes from this flexibility provided by the pulse sequence. We will now present a brief derivation of the coherence function $\chi(t)$ which generically characterizes the decay of coherence in a qubit subject to dephasing noise and a given pulse sequence. The notation takes inspiration from [8].

We define our coherence amplitude by $|\langle\sigma_+\rangle|$, where $\sigma_+ = (\sigma_x + i\sigma_y)/2$ is the qubit raising operator. In analogy to a spin-1/2 system, $|\langle\sigma_+\rangle|$ gives the transverse (xy-plane) polarization of the Bloch vector. If there is no well-defined phase between the ground and excited states of the qubit, $|\langle\sigma_+\rangle| = 0$.

Given a qubit density operator $\rho(t) = |\Psi(t)\rangle\langle\Psi(t)|$, we have $|\langle\sigma_+\rangle| = |\mathrm{Tr}\{\sigma_+\rho(t)\}| = |\rho_{01}(t)|$. In order to acknowledge the distribution of noise amplitudes, we calculate the evolution of the density operator by

$$\rho(t) = \sum_\eta p(\eta) U_\eta(t)\rho(0)U_\eta^\dagger(t), \tag{6}$$

where $U_\eta(t)$ is the time evolution operator with noise realization $\eta(t)$, and $p(\eta)$ gives the probability of $\eta(t)$.

We can now express the total coherence amplitude as the average over all noise realizations, giving noise realization $\eta(t)$ a weight $p(\eta)$,

$$\langle\sigma_+\rangle = \sum_\eta p(\eta)\langle\sigma_+\rangle_\eta, \tag{7}$$

$$\langle\sigma_+\rangle_\eta = \mathrm{Tr}\left\{\sigma_+ U_\eta(t)\rho(0)U_\eta^\dagger(t)\right\}. \tag{8}$$

Focusing on one realization, we can express the time evolution operator as

$$U_\eta(t) = \exp\left[-\frac{i}{\hbar}\int_0^t H(t')\,dt'\right] \tag{9}$$

$$= \exp\left[-\frac{i}{2}\sigma_z\int_0^t \omega(t')\,dt'\right], \tag{10}$$

$$\omega(t) = \omega_0 + \eta(t). \tag{11}$$

If we interrupt the evolution with a π-pulse given by $U_\pi = \exp[-i\sigma_x/2\cdot\pi] = -i\sigma_x$, it flips the phase accumulated by each state. Explicitly, assume the unitary evolution from $t = 0$ to $t = t_1$ takes the form $U^1 = \exp[-i\phi_1\sigma_z]$, and the unitary evolution from $t = t_1$ to $t = t_2$ is given by $U^2 = \exp[-i\phi_2\sigma_z]$. The total evolution takes the form

$$U^2U^1 = e^{-i\phi_2\sigma_z}e^{-i\phi_1\sigma_z} = e^{-i(\phi_2+\phi_1)\sigma_z}. \tag{12}$$

If we interrupt the evolution with a π-pulse instantaneously at t_1, we instead have

$$U^2U_\pi U^1 = e^{-i\phi_2\sigma_z}(-i\sigma_x)e^{-i\phi_1\sigma_z} = -ie^{-i(\phi_2-\phi_1)\sigma_z}. \tag{13}$$

By applying a series of N π-pulses at times $t_1, \cdots, t_N$, we can define a modulation function $s(t)$ which switches between +1 and -1 at each t_i to capture the modulation of the phase. Letting U^i be the evolution from t_{i-1} to t_i, $t_0 = 0$, and $t_{N+1} = t$, the qubit evolves with

$$U_\eta(t) = U_\eta^{N+1}U_\pi U_\eta^N \cdots U_\pi U_\eta^1 \tag{14}$$

$$= (-i)^N \exp\left[-\frac{i}{2}\sigma_z\sum_{i=0}^{i=N}\int_{t_i}^{t_{i+1}} s(t')\omega(t')\,dt'\right] \tag{15}$$

$$= (-i)^N \exp\left[-\frac{i}{2}\sigma_z\int_0^t s(t')\omega(t')\,dt'\right]. \tag{16}$$

We note that $\sigma_+\exp[-i\phi\sigma_z] = \exp[i\phi\sigma_z]\sigma_+$ such that $\sigma_+U_\eta(t) = U_\eta^\dagger(t)\sigma_+$. Calculating the coherence amplitude with noise realization $\eta(t)$ from Eq. 8 then yields

$$\langle\sigma_+\rangle_\eta = \mathrm{Tr}\left\{\sigma_+U_\eta(t)\rho(0)U_\eta^\dagger(t)\right\} \tag{17}$$

$$= \mathrm{Tr}\left\{U_\eta^\dagger(t)U_\eta^\dagger(t)\sigma_+\rho(0)\right\} \tag{18}$$

$$= (-i)^{2N}\exp\left[-i\int_0^t s(t')\omega(t')\,dt'\right]\mathrm{Tr}\left\{\sigma_+\rho(0)\right\}. \tag{19}$$

Assuming a state prepared on the equator of the Bloch sphere, $\mathrm{Tr}\{\sigma_+\rho(0)\} = 1/2$. We can split $\omega(t)$ into its constituents ω_0 and $\eta(t)$, where the constant term ω_0 will lead to a phase prefactor $e^{-i\phi}$. When the magnitude is taken, this term, along with the $(-i)^{2N}$, will vanish.

In order to consider the ensemble of noise realizations, we must make assumptions about the statistics of the amplitudes $\eta(t)$ from measurement to measurement. As detailed in the previous section, this is not necessarily related to the dynamics of the noise $G(\tau)$. A natural approximation here is to consider the noise amplitudes as Gaussian-distributed. This can be justified in many cases by arguing that the noise $\eta(t)$ derives from the sum over many dynamical degrees of freedom, and thus the central limit theorem guarantees the distribution of this sum to be Gaussian [8]. To be explicit, with $\Delta^2 \equiv \langle\eta(t)^2\rangle$ as the variance with respect to the environment degrees of freedom, we have

$$P(\eta(t) = \eta) = \frac{1}{\sqrt{2\pi\Delta^2}}\exp\left[-\frac{\eta^2}{2\Delta^2}\right]. \tag{20}$$

Ignoring the constant phase factors in Eq. 19 and defining $X(t) = \int_0^t s(t')\eta(t')dt'$, Eq. 7 becomes

$$\langle \sigma_+ \rangle \propto \sum_\eta p(\eta) \exp\left[-i\int_0^t s(t')\eta(t')\,dt'\right] \tag{21}$$

$$\propto \langle\!\langle e^{-iX(t)} \rangle\!\rangle, \tag{22}$$

where $\langle\!\langle\cdot\rangle\!\rangle$ represents the ensemble average over noise processes. One must evaluate a Gaussian functional integral to perform this ensemble average. At the risk of irony, this calculation is especially tedious, so we refer the reader to other sources for details on these types of calculations [8–10]. One finds an elegant result by introducing a filter function based on the modulation $s(t)$,

$$F(t,\omega) = \frac{\omega^2}{2}\left|\int_0^t dt' s(t') e^{i\omega t'}\right|^2, \tag{23}$$

such that we arrive at a normalized coherence $W(t)$:

$$W(t) \equiv \frac{|\rho_{01}(t)|}{|\rho_{01}(0)|} = e^{-\chi(t)}, \tag{24}$$

$$\chi(t) = \frac{1}{\pi}\int_0^\infty S(\omega)\frac{F(t,\omega)}{\omega^2}\,d\omega. \tag{25}$$

This is the central result: the coherence function $\chi(t)$. This function generically captures the decay of coherence of a qubit subject to dephasing noise with a power spectrum $S(\omega)$ under the influence of a given modulation $s(t)$ and corresponding filter function $F(t,\omega)$.

The expression Eq. 25 serves as a powerful tool for exploring and exploiting the environmental noise $S(\omega)$. For example, the coherence $W(t)$ of the qubit can be measured under the control of different pulse-sequences, which yields information about the environmental noise spectrum [1]. Or, one could design pulse-sequences such that the coherence $W(t)$ is more (less) sensitive to noise at different frequencies, which has applications to noise spectroscopy (quantum information processing) [9]. The use of pulse sequences to decouple a qubit from decohering noise is known as dynamical decoupling, and has enabled long-lived coherence in solid-state qubits [11].

Tabulations of filter functions for common pulse sequences can be found in many sources, for example [9]. We find it instructive to show some common examples of modulations, their derived filter functions, and the corresponding coherence decays when exposed to different environmental noise spectra, in Fig. 1.

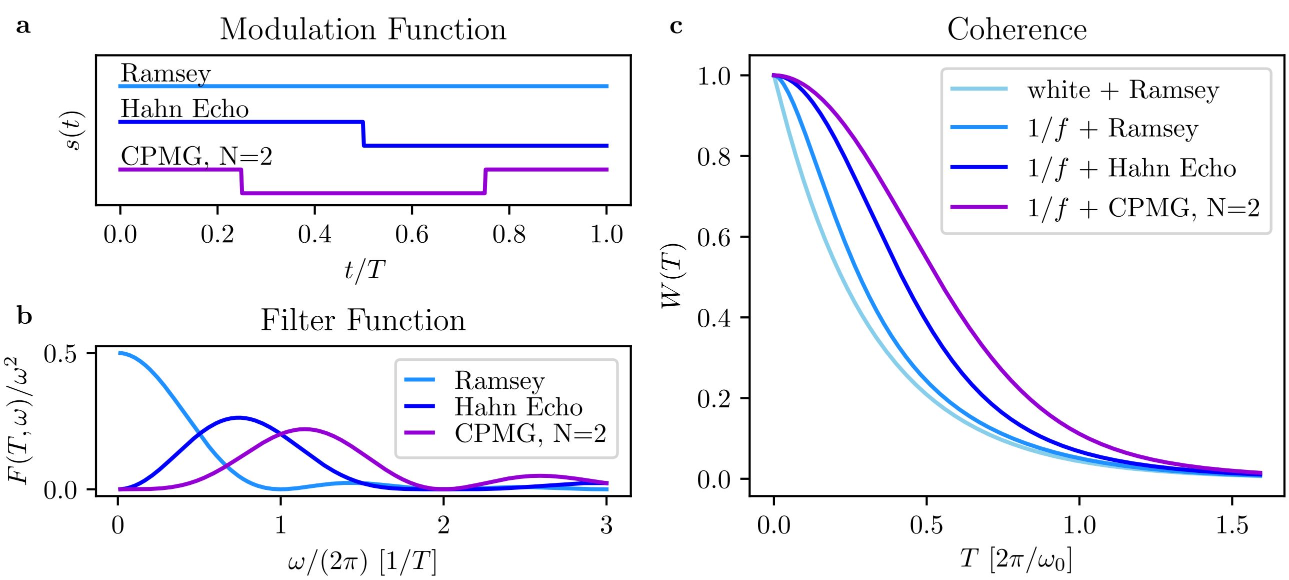

FIG. 1. (a) Ramsey (Free-Induction-Decay), Hahn (Spin) Echo, and Carr–Purcell–Meiboom–Gill (CPMG) modulation functions over an experiment of duration T. (b) Corresponding filter functions for the modulations given in (a). Frequencies on the x-axis are given in units of the total experiment time T. The Ramsey filter function is most sensitive to noise at $\omega = 0$, and reaches minima when the period of the noise $2\pi/\omega$ is an integer multiple of the experiment time T. The CPMG filter function pushes the noise envelope further out as N increases. (c) Coherences of experiments with given modulation function and noise power spectrum. For white noise, $S_w(\omega) = \omega_0$. For $1/f$ noise, $S_{1/f}(\omega \geq \omega_0) = \omega_0^2/\omega$ and $S_{1/f}(\omega < \omega_0) = \omega_0$.

Unfortunately, the assumptions made in this formalism of pure dephasing noise with Gaussian amplitudes will not describe every system. Methodologies for exploring non-Gaussian noise are the subject of current research [3], with the first experimental realization in 2019 [12]. We also note that the presented filter-function approach to noise spectroscopy is limited by the ability to design clever pulse sequences, and has been found to be most helpful in exploring low-frequency ranges of $S(\omega)$. An alternative tool for exploring the noise spectra is provided by preparing the qubit in a state and monitoring the relaxation from that state. This approach, termed "relaxometry," typically provides access to $S(\omega)$ at higher frequencies [1, 3, 5]. For example, by exploring the relaxation from the excited state to the ground state, $S(\omega)$ can be probed near the qubit energy splitting, which for NVs and superconducting qubits can be in the GHz range.

C. 1/f Noise

In numerous physical systems, environmental noise which scales as $S(\omega) \propto 1/\omega$ has been observed. Due to it's ubiquity, we present this brief note offering a simple model for how such a spectrum can arise, inspired by [9].

Consider a random telegraph signal (RTS) $f(t)$ flipping between $+v/2$ and $-v/2$ with an average rate γ. The correlation function and corresponding PSD are given by

$$G^{\gamma}_{\mathrm{RTS}}(\tau) = \langle f(t+\tau)f(t)\rangle = \frac{v^2}{4}e^{-2\gamma\tau}, \tag{26}$$

$$S^{\gamma}_{\mathrm{RTS}}(\omega) = \frac{v^2\omega}{\omega + 4\gamma^2}. \tag{27}$$

If we now consider a distribution of switching rates γ with probability $p(\gamma) \propto 1/\gamma$, the average lineshape is

$$S_{\mathrm{RTS}}(\omega) = \int_0^{\infty} S^{\gamma}_{\mathrm{RTS}}(\omega)\, p(\gamma)\, d\gamma \propto \frac{v^2}{\omega}. \tag{28}$$

Thus, the question becomes where one can find such an ensemble of random telegraphs. One relevant example to today's quantum technologies is the ensemble of atomic tunneling sites in amorphous solids. These sites can be understood as effective two-level systems comprised of localized states in a double-well potential [13], where the tunneling rate is exponentially suppressed by the barrier height. Assuming a uniform distribution of barrier heights, the tunneling rates take on a log-uniform distribution $p(\gamma) \propto 1/\gamma$ [9].

Due to use of amorphous aluminum oxide tunnel barriers in superconducting qubit Josephson Junctions, as well as the rapid formation of native oxides on the surfaces of electrodes when exposed to ambient conditions, these systems are commonplace on many interfaces of superconducting circuits [2, 4]. Another potential example is the amorphous surface terminations of diamonds hosting NV centers, where it has been recently shown that the surface morphology affects the coherence [14].

III. APPLICATIONS OF NOISE SPECTROSCOPY VIA FILTER FUNCTIONS

A. NV Centers

NV centers are point-like defects in diamond that constitute a promising platform for magnetic imaging, electron spin resonance, quantum memory, and quantum information processing [1, 5, 15, 16]. They have a spin-1 level structure with a zero-field splitting of 2.88-GHz between the $m = 0$ and $m = \pm 1$ states. One can choose two of the three levels to realize a qubit system. The $m = 0$, $m = \pm 1$ levels comprise the "single-quantum" (SQ) basis, which is dependent on the zero-field splitting. The $m = -1$, $m = +1$ levels comprise the "double-quantum" (DQ) basis, which is independent of the zero-field splitting and twice as sensitive to applied magnetic fields.

Understanding the noise spectra seen by NVs will allow for the optimization of their properties for specific applications. We present a recent result using the formalism presented in the previous section which elucidates the relationship between NV depth and observed noise.

Consider $\chi(t)$ defined in Eq. 25. If one uses a filter function $F(t,\omega)/\omega^2 = \delta(\omega - \omega_0)t$, then the spectrum can be extracted as $S(\omega_0) = -\pi \ln[W(t)]/t$. By using CPMG sequences with different numbers of pulses N to approximate such a filter function, the noise spectra of several NVs were extracted from the coherences in [6]. The results are presented in Fig. 2. The spectra were fitted with a sum of two zero-mean Lorentzians with different coupling strengths (Δ_i) and correlation times ($\tau_{c(i)}$):

$$S(\omega) = \sum_{i=1,2} \frac{\Delta_i^2 \tau_{c(i)}}{\pi} \frac{1}{1 + (\omega\tau_{c(i)})^2} \tag{29}$$

By mapping the spectra of several NVs at different depths, the correlation times were found to be constant, but the coupling strengths were found to decrease with depth d. Specifically, the low-frequency coupling strength followed a power law $\Delta_{low-f} \propto 1/d^{1.75}$, and the high-frequency coupling strength followed a power law $\Delta_{high-f} \propto 1/d^{0.9}$. As an electronic spin bath is predicted to provide a coupling strength of $1/d^2$, the low-frequency noise could be reasonably assigned to this mechanism. The high-frequency noise was attributed to surface-modified phononic coupling. The identification of the electronic spin bath noise has led to successful efforts to decouple shallow NVs from such noise, employing techniques such as resonant driving [15, 16].

B. Superconducting Qubits

Superconducting circuits offer another promising solid-state qubit platform. Due to the nature of the devices, the circuit interfaces with large surface areas host many defects that provide decohering noise. We feature a study of the noise spectrum seen by a flux qubit obtained by

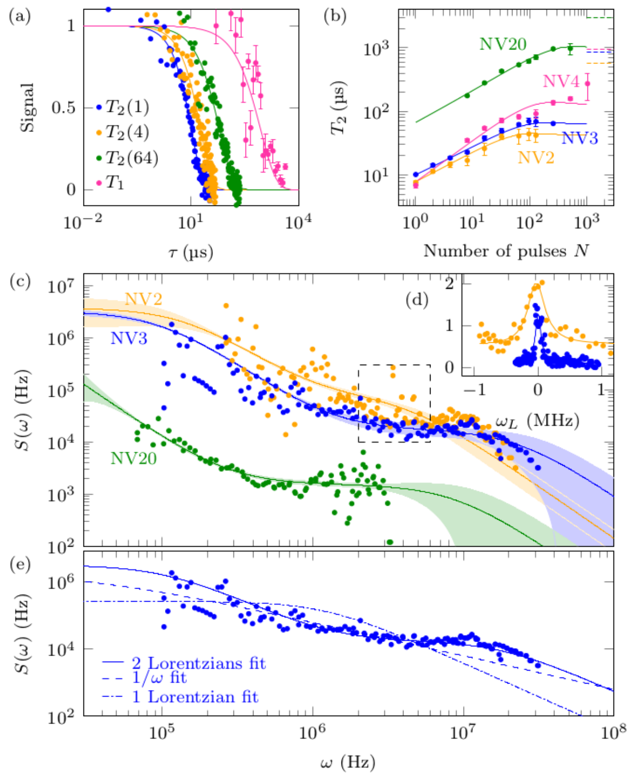

FIG. 2. Reproduced from [6]. (a) Coherence $W(t)$ and energy relaxation for an NV at an approximated depth of 3 nanometers. $T_2(N)$ denotes driving with a CPMG sequence of N pulses. T_1 denotes a longitudinal relaxation measurement. (b) Coherence time T_2 as a function of N. Saturation is a consequence of unsuppressed high frequency noise. (c) Noise spectra $S(\omega)$ extracted by spectral decomposition for three different NVs, labelled by their depth in nanometers. Fits used a sum of two Lorentzians. 1σ confidence intervals are given by the shaded regions. (d) Noise at the Hydrogen Larmor frequency ($x = 0$) in relative units. (e) Fits of $S(\omega)$ for NV3 (3 nm depth) with different spectral functions.

dynamical decoupling [17]. The Hamiltonian of the flux qubit system with splitting $\omega_{01} = \sqrt{\epsilon^2 + \Delta^2}$ is given by

$$H = -\frac{\hbar}{2}\left[(\epsilon + \delta\epsilon)\sigma_x + (\Delta + \delta\Delta)\sigma_z\right]. \tag{30}$$

In this study, the filter function was also created with CPMG pulse sequences. By assuming a noise coupling strength γ and a sufficiently narrow filter function such that the noise was constant within bandwidth B, the spectrum was calculated with

$$\chi(t) \approx \gamma^2 S(\omega) F(\omega)/\omega^2 \cdot B. \tag{31}$$

The bandwidth B and frequency ω were calculated numerically for each pulse sequence.

The noise spectrum at higher frequencies was calculated using energy relaxation via Fermi's golden-rule: $\Gamma_1 = \pi/2S(\omega_{01})$, and driven-relaxation techniques were used to generate validating approximations of the spectrum. The noise spectrum was found to follow a $1/f^{0.9}$ power law for frequencies below the bare qubit frequency $\Delta/2\pi$, and displayed an increase characteristic of Nyquist noise at higher frequencies.

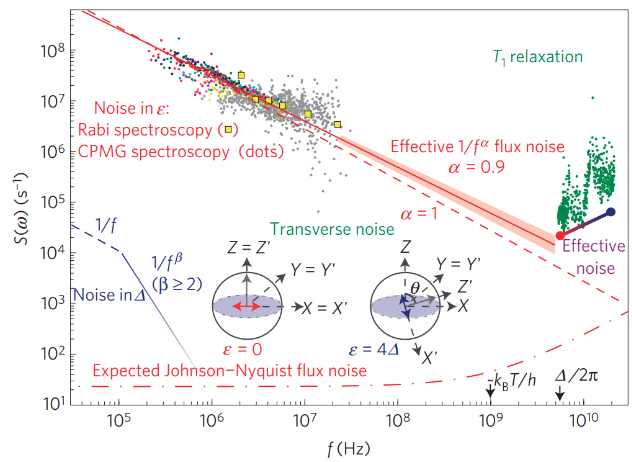

FIG. 3. Reproduced from [17]. Multicolored dots represent data from CPMG $\delta\epsilon$ noise spectroscopy, where the colors represent the number of pulses N up to $N = 250$. Yellow squares represent data from Rabi (driven) $\delta\epsilon$ noise spectroscopy. Diagonal dashed lines represent estimated ϵ (red) and Δ (blue) $1/f$ noise. The solid red line is the fitted power dependence $1/f^{0.9}$. Green dots represent T_1 relaxation data, which turns from pure $\delta\epsilon$ noise at $\Delta/2\pi$ to pure $\delta\Delta$ noise at higher frequencies. This is denoted by the colored red/blue circles in the purple line, which follows the increasing Nyquist noise. The dash-dotted line shows the expected thermal and Nyquist noise. The insets show the Bloch picture of the quantization axes, where ϵ points in the X direction, and Δ in the Z direction, and the red/blue arrows denote transverse noise.

This study demonstrated the ability of CPMG sequences to suppress low-frequency $1/f$ noise by pushing the dephasing time to the $T_2 \approx 2T_1$ limit. By confronting this limitation of T_1, the goal became identifying the responsible energy relaxation processes. This is an active area of research, some recent exciting results being achieved by more closely monitoring and varying the properties of the materials used in such devices [18].

IV. OUTLOOK

The precise design and control of quantum systems has enabled groundbreaking research and technologies in recent years [1, 3]. In order to reach the fundamental limits of such systems, the ability to suppress unwanted parasitic environmental couplings will be of singular importance. The suppression of such couplings necessitates understanding the origin of the leading-order interactions. In many cases, and especially in the solid-state, this poses a serious challenge since many-body phenomena can give rise to arbitrarily complex physics. When relating the microscopic interactions to a quantity such as the noise power spectrum, analytical expressions are only obtained through unreserved approximation.

However, by mapping the spectrum of a quantum two-level system with noise spectroscopy, insights about the origins of such couplings can be found. Thus, the ability to extract the noise spectrum is a crucial first step. We presented the well-established formalism which relates a pure dephasing noise power spectrum to the coherence of a qubit given Gaussian-distributed noise amplitudes. The study of non-Gaussian noise spectra is an active area of research [1, 3, 12], as is study of relaxation during free and driven evolution [1]. With these approaches and more, we are optimistic about the near-term advancement of quantum device engineering which will enable the next generation of platforms for research and technology at the frontiers of quantum physics.

ACKNOWLEDGMENTS

We thank the reader for making it all the way through. We also thank Wolfgang Ketterle and the TAs of 8.421 for providing an engaging and informative introduction to AMO.

[1] C. L. Degen, F. Reinhard, and P. Cappellaro, Quantum sensing, Reviews of Modern Physics **89**, 035002 (2017), arXiv: 1611.02427.

[2] J. Lisenfeld, A. Bilmes, A. Megrant, R. Barends, J. Kelly, P. Klimov, G. Weiss, J. M. Martinis, and A. V. Ustinov, Electric field spectroscopy of material defects in transmon qubits, npj Quantum Information **5**, 105 (2019).

[3] P. Krantz, M. Kjaergaard, F. Yan, T. P. Orlando, S. Gustavsson, and W. D. Oliver, A Quantum Engineer's Guide to Superconducting Qubits, Applied Physics Reviews **6**, 021318 (2019), arXiv: 1904.06560.

[4] C. Müller, J. H. Cole, and J. Lisenfeld, Towards understanding two-level-systems in amorphous solids: insights from quantum circuits, Reports on Progress in Physics **82**, 124501 (2019).

[5] L. T. Hall, P. Kehayias, D. A. Simpson, A. Jarmola, A. Stacey, D. Budker, and L. C. L. Hollenberg, Detection of nanoscale electron spin resonance spectra demonstrated using nitrogen-vacancy centre probes in diamond, Nature Communications **7**, 1 (2016), number: 1 Publisher: Nature Publishing Group.

[6] Y. Romach, C. Müller, T. Unden, L. Rogers, T. Isoda, K. Itoh, M. Markham, A. Stacey, J. Meijer, S. Pezzagna, B. Naydenov, L. McGuinness, N. Bar-Gill, and F. Jelezko, Spectroscopy of Surface-Induced Noise Using Shallow Spins in Diamond, Physical Review Letters **114**, 017601 (2015), publisher: American Physical Society.

[7] G. Gordon, N. Erez, and G. Kurizki, Universal dynamical decoherence control of noisy single- and multi-qubit systems, Journal of Physics B: Atomic, Molecular and Optical Physics **40**, S75 (2007).

[8] M. Fanciulli, C. E. Ascheron, and A. H. Duhm, eds., *Electron Spin Resonance and Related Phenomena in Low-Dimensional Structures*, Topics in Applied Physics, Vol. 115 (Springer Berlin Heidelberg, Berlin, Heidelberg, 2009).

[9] Cywiński, R. M. Lutchyn, C. P. Nave, and S. Das Sarma, How to enhance dephasing time in superconducting qubits, Physical Review B **77**, 174509 (2008).

[10] J. L. Skinner and D. Hsu, Pure dephasing of a two-level system, The Journal of Physical Chemistry **90**, 4931 (1986).

[11] J. T. Muhonen, J. P. Dehollain, A. Laucht, F. E. Hudson, R. Kalra, T. Sekiguchi, K. M. Itoh, D. N. Jamieson, J. C. McCallum, A. S. Dzurak, and A. Morello, Storing quantum information for 30 seconds in a nanoelectronic device, Nature Nanotechnology **9**, 986 (2014).

[12] Y. Sung, F. Beaudoin, L. M. Norris, F. Yan, D. K. Kim, J. Y. Qiu, U. von Lüpke, J. L. Yoder, T. P. Orlando, S. Gustavsson, L. Viola, and W. D. Oliver, Non-Gaussian noise spectroscopy with a superconducting qubit sensor, Nature Communications **10**, 3715 (2019).

[13] G. J. Grabovskij, T. Peichl, J. Lisenfeld, G. Weiss, and A. V. Ustinov, Strain Tuning of Individual Atomic Tunneling Systems Detected by a Superconducting Qubit, Science **338**, 232 (2012).

[14] S. Sangtawesin, B. L. Dwyer, S. Srinivasan, J. J. Allred, L. V. Rodgers, K. De Greve, A. Stacey, N. Dontschuk, K. M. O'Donnell, D. Hu, D. A. Evans, C. Jaye, D. A. Fischer, M. L. Markham, D. J. Twitchen, H. Park, M. D. Lukin, and N. P. de Leon, Origins of Diamond Surface Noise Probed by Correlating Single-Spin Measurements with Surface Spectroscopy, Physical Review X **9**, 031052 (2019).

[15] D. Bluvstein, Z. Zhang, C. A. McLellan, N. R. Williams, and A. C. B. Jayich, Extending the Quantum Coherence of a Near-Surface Qubit by Coherently Driving the Paramagnetic Surface Environment, Physical Review Letters **123**, 146804 (2019).

[16] E. Bauch, C. A. Hart, J. M. Schloss, M. J. Turner, J. F. Barry, P. Kehayias, S. Singh, and R. L. Walsworth, Ultralong Dephasing Times in Solid-State Spin Ensembles via Quantum Control, Physical Review X **8**, 031025 (2018).

[17] J. Bylander, S. Gustavsson, F. Yan, F. Yoshihara, K. Harrabi, G. Fitch, D. G. Cory, Y. Nakamura, J.-S. Tsai, and W. D. Oliver, Noise spectroscopy through dynamical decoupling with a superconducting flux qubit, Nature Physics **7**, 565 (2011).

[18] A. P. M. Place, L. V. H. Rodgers, P. Mundada, B. M. Smitham, M. Fitzpatrick, Z. Leng, A. Premkumar, J. Bryon, S. Sussman, G. Cheng, T. Madhavan, H. K. Babla, B. Jaeck, A. Gyenis, N. Yao, R. J. Cava, N. P. de Leon, and A. A. Houck, New material platform for superconducting transmon qubits with coherence times exceeding 0.3 milliseconds, arXiv:2003.00024 [cond-mat, physics:physics, physics:quant-ph] (2020), arXiv: 2003.00024.